Investigating Beeman, Euler-Cromer, and Direct Euler Methods
for Many-Body Orbital Simulations: A Case Study of the Solar System

Mehul Bandhu
Computer Simulation (PHYS08026), University of Edinburgh
April 8, 2025

1 Introduction

Many-body dynamics are of central importance in astrophysics and molecular dynamics. Accurate simulation of complex systems is essential for both predictive modeling and fundamental research. This project evaluates the effectiveness of Euler, Euler-Cromer, and Beeman methods in simulating the motion of bodies in the Solar System.

The necessity of this work is underscored by the challenges encountered when simulating systems with large numbers of interacting bodies. In such cases, not only does computational time become a significant constraint, but maintaining accuracy and conserving physical quantities such as energy also become critical. The performance of an integration method depends strongly on simulation parameters, and small differences can lead to large deviations over time. An in-depth study has been carried out to examine how energy conservation, and numerical accuracy vary across different integration techniques, providing a reliable basis for selecting the most suitable method based on both physical fidelity and available computational resources.

Several experiments have been conducted, including the prediction of orbital periods, analysis of planetary alignments, and long-term tracking of total system energy. These tests not only validate the physical realism of the simulations but also highlight the trade-offs between accuracy and computational cost across different methods. Particular attention is given to how error accumulates over time and how simulation parameters influence performance.

2 Methods

2.1 Numerical Framework and Design

This project simulates the gravitational interactions among multiple celestial bodies (the Sun and various planets) using an object-oriented approach in Python. Each *Body* in the simulation stores physical properties such as position, velocity, and mass, as well as instantaneous and previous accelerations. *Simulation* class contains the main numerical routines, including reading input parameters, updating body positions and velocities, calculating energies, and detecting events such as orbit completions and planetary alignments.

2.2 Initialization

Input data (planetary masses, initial orbital radii, the gravitational constant, etc.) are provided in a JSON file. Each planet is placed on the $+x$ axis at $(r, 0)$, where r is its orbital radius. If $r > 0$, the planet is given an initial velocity along the $+y$ axis, following

$$v = \sqrt{\frac{GM_{\text{sun}}}{r}}, \tag{1}$$

assuming near-circular orbits. The Sun is placed at the origin with zero initial velocity.

2.3 Acceleration and Integration Methods

At each time step Δt, the pairwise gravitational accelerations are computed: for bodies i and j,

$$\mathbf{a}_i = -G \frac{m_j}{\|\mathbf{r}_{ij}\|^3} \mathbf{r}_{ij}, \tag{2}$$

where $\mathbf{r}_{ij} = \mathbf{r}_i - \mathbf{r}_j$ and $\|\mathbf{r}_{ij}\|$ is the Euclidean distance. Contributions from all other bodies are summed to obtain the total acceleration on body i.
Three numerical schemes – Direct Euler, Euler-Cromer, and Beeman, are implemented:

Direct Euler

$$\mathbf{r}(t+\Delta t) = \mathbf{r}(t) + \mathbf{v}(t)\,\Delta t, \tag{3}$$
$$\mathbf{v}(t+\Delta t) = \mathbf{v}(t) + \mathbf{a}(t)\,\Delta t. \tag{4}$$

Euler-Cromer

$$\mathbf{v}(t+\Delta t) = \mathbf{v}(t) + \mathbf{a}(t)\,\Delta t, \tag{5}$$
$$\mathbf{r}(t+\Delta t) = \mathbf{r}(t) + \mathbf{v}(t+\Delta t)\,\Delta t. \tag{6}$$

Beeman

$$\mathbf{r}(t+\Delta t) = \mathbf{r}(t) + \mathbf{v}(t)\,\Delta t + \frac{1}{6}\big[4\,\mathbf{a}(t) - \mathbf{a}(t-\Delta t)\big]\Delta t^2, \tag{7}$$
$$\mathbf{v}(t+\Delta t) = \mathbf{v}(t) + \frac{1}{6}\Big[2\,\mathbf{a}(t+\Delta t) + 5\,\mathbf{a}(t) - \mathbf{a}(t-\Delta t)\Big]\Delta t. \tag{8}$$

Equations 3 – 8 are taken from the project documentation.

Beeman is the primary choice for its enhanced energy conservation properties. Euler and Euler-Cromer are tested for comparison.
A key assumption is that the system remains at equilibrium at $t = 0$, so the acceleration does not jump discontinuously from the moment before the simulation starts ($t < 0$) to the first step ($t = 0$). Hence, it is natural to set $\mathbf{a}(0 - \Delta t) = \mathbf{a}(0)$ when initializing the integrator.

2.4 Orbital Periods and Alignments

To detect orbital periods, each planet's angular position $\theta = \tan^{-1}(y/x)$ is tracked over time. Upon accumulating a net change of 2π, the code logs a completed orbit and records the time of first completion as that planet's orbital period. Planetary alignments are detected by computing each planet's orbital angle and checking whether all inner planets lie within a specified angular range (e.g. $\pm 5°$) around the mean of their angles.

2.5 Energy Computation

At each iteration, kinetic energy $K_i = \frac{1}{2} m_i \|\mathbf{v}_i\|^2$ and pairwise potential energy $U_{ij} = -G \frac{m_i m_j}{\|\mathbf{r}_{ij}\|}$ are computed for each pair of bodies, yielding a total energy

$$E = \sum_i K_i + \sum_{i \neq j} U_{ij}. \tag{9}$$

Monitoring E over long simulation spans indicates whether the integrator conserves energy or drifts significantly.

2.6 Time Step Variation

Simulations are repeated with different Δt values to compare orbital period deviations, alignment times, and energy conservation. This highlights the trade-off between lower computational cost (larger Δt) and higher accuracy (smaller Δt).

3 Results

In this section, the outcomes of the simulations performed using Beeman's method is shown. These results are further compared with Direct Euler and Euler-Cromer methods using certain key metrics. Key metrics include orbital periods, energy conservation over time, relative computation times, and effect of perturbations on the periods. Finally, additional statistics on planetary alignments are displayed using Beeman's method.

3.1 Orbital Period using Beeman's Method

For each planet, the simulation was run over a 2000-year period and the orbital period was recorded for each completed orbit. The final reported value is the mean orbital period, with its standard deviation quantifying the numerical fluctuations. Table 1 lists the reference orbital period T_{ref}, the mean simulated orbital period T_{sim}, (the standard deviation σ, and the percentage error $\Delta_{\%}$ (computed as $100 \times (\Delta_{\text{abs}}/T_{\text{ref}})$). All values are rounded to three decimal places. Here, Δ_{abs} is calculated as the absolute difference between the simulated mean and the reference period, i.e., $\Delta_{\text{abs}} = |T_{\text{sim}} - T_{\text{ref}}|$.

Table 1: Mean Orbital Periods and Errors obtained with Beeman's method for the major planets (in years).

Planet	T_{ref}	T_{sim}	σ	$\Delta_{\%}$
Mercury	0.241	0.241	0.001	0.0%*
Venus	0.615	0.614	0.001	0.163%
Earth	1.000	0.999	0.001	0.1%
Mars	1.880	1.879	0.002	0.053%
Jupiter	11.900	11.805	0.015	0.798%
Saturn	29.400	29.001	0.007	1.357%
Uranus	84.700	83.012	0.004	1.991%
Neptune	163.700	162.622	0.010	0.658%

(*) The 0.0% error is due to rounding; the actual error is nonzero, but falls below the reporting precision. *T_{ref}–NASA fact sheet*

As the standard deviations are around 0.01 years for most of the planets, this confirms that the orbits remain stable over long periods, as expected. Furthermore, the percentage errors for all planets except Uranus and Saturn are below 1%, which underscores the high accuracy of the numerical simulations.

3.2 Energy Conservation

To assess the **energy conservation properties**, the total mechanical energy of the system,

$$E(t) = \sum_i \tfrac{1}{2} m_i \|\mathbf{v}_i(t)\|^2 + \sum_{i<j} \Big(-G \frac{m_i m_j}{\|\mathbf{r}_{ij}(t)\|}\Big),$$

was tracked over the duration of each simulation. Oscillation of the total energy (TE) was observed in cases of each of planets over the duration. This effect was more apparent for the Beeman and Euler-Cromer methods.

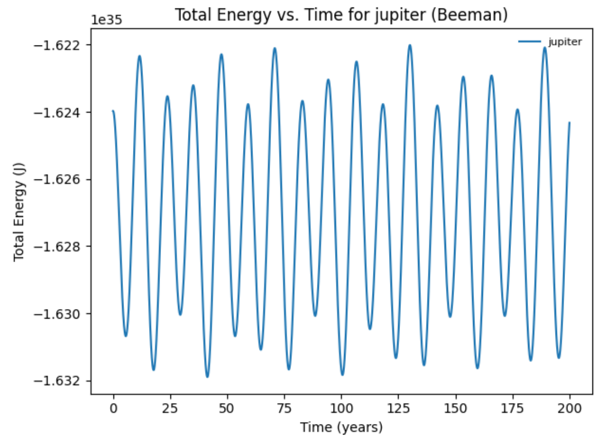

Figure 1: Change in total energy of Jupiter with time.

Beeman shows energy stability, with $< 0.5\%$ variation over long intervals.

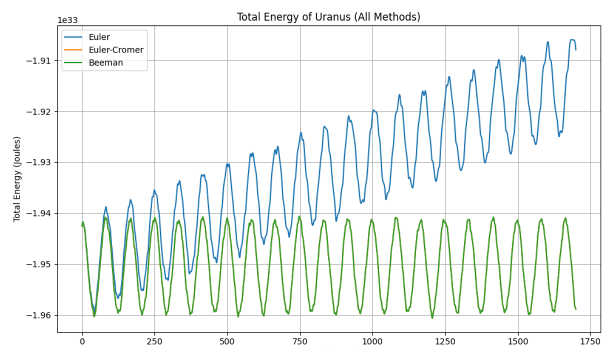

Figure 2: Energy Conservation characteristics over period of simulations for various numerical methods. Euler-Cromer energy curve overlaps with the Beeman curve.

As seen in Figure 2, the Euler method accumulates systematic error over time which leads to a drift in TE. This drift is more pronounced in case of inner planets – which has been discussed in detail in the following section.

To assess the numerical stability and energy conservation properties of each integration method quantitatively (Euler, Euler-Cromer, Beeman), two key metrics were computed from the simulation results: the *energy drift* and the *energy oscillation*.

Energy Drift is calculated as the maximum percentage deviation of the total energy $E(t)$ from its initial value $E(0)$:

$$\text{Energy Drift } (\%) = \frac{\max |E(t) - E(0)|}{|E(0)|} \times 100. \tag{10}$$

Table 2: Energy Drift and Oscillation over 2000 years for different numerical methods (Time step = 0.001 years)

Planet	**Euler**		**Euler-Cromer**		**Beeman**	
	Drift (%)	Oscillation (%)	Drift (%)	Oscillation (%)	Drift (%)	Oscillation (%)
Sun	35.2926	8.8164	0.2008	0.0593	0.1872	0.0570
Mercury	98.3369	4.9980	0.2004	0.0634	0.1356	0.0609
Venus	104.9100	11.3110	0.1877	0.0815	0.1874	0.0843
Earth	111.1835	15.2022	0.2285	0.0993	0.2284	0.1003
Mars	346.9050	134.3910	0.2972	0.1271	0.2974	0.1274
Jupiter	36.0915	9.7517	0.4916	0.1778	0.4917	0.1779
Saturn	12.8943	3.4001	0.6500	0.2437	0.6500	0.2437
Uranus	1.8813	0.6367	0.9316	0.3327	0.9316	0.3327
Neptune	1.1243	0.4422	1.1569	0.4148	1.1569	0.4148

This metric quantifies long-term systematic deviations of energy from the initial (reference) value over the entire simulation period. **Energy Oscillation** captures the magnitude of short-term fluctuations around the mean energy, normalized by the initial energy:

$$\text{Energy Oscillation (\%)} = \frac{\sigma\left(E(t)\right)}{|E(0)|} \times 100, \tag{11}$$

where $\sigma(E(t))$ denotes the standard deviation of the total energy over the full simulation.

The results presented in Table 2 clearly demonstrate that the Euler method shows significantly higher energy drift and oscillations, particularly pronounced for inner planets such as Mercury, Venus, Earth, and Mars. In contrast, the Euler-Cromer and Beeman methods yield minimal energy drift and oscillation, reflecting their superior numerical stability and improved energy conservation over long integration periods.

Furthermore, it was observed that the energy drift for inner planets is greater for the Euler-Cromer method compared to the Beeman method; a similar trend was noted for energy oscillations. This suggests that energy is better conserved, and orbital stability maintained over longer periods, by the Beeman method, as expected.

3.3 Orbital Period Comparison

To visualize and compare the results of the orbital period for each integration method, simulations were run for 2.0×10^5 iterations with $\Delta t = 0.001$ years.

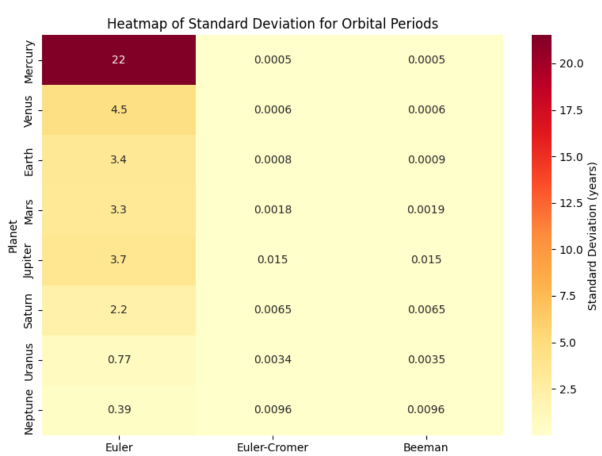

Figure 3: Heatmap of Standard Deviations for Orbital Periods.

Two heat maps were generated: one for the standard deviations of the orbital periods (Figure 3) and one for the percentage errors relative to the values accepted/known in the literature (Figure 4).

Lighter shades indicate smaller standard deviations, reflecting more stable orbits over the simulation period. Euler-Cromer and Beeman methods produced highly stable orbits over the period of simulation, whereas Direct Euler method failed to produce consistent result and a drift in orbital periods was observed.

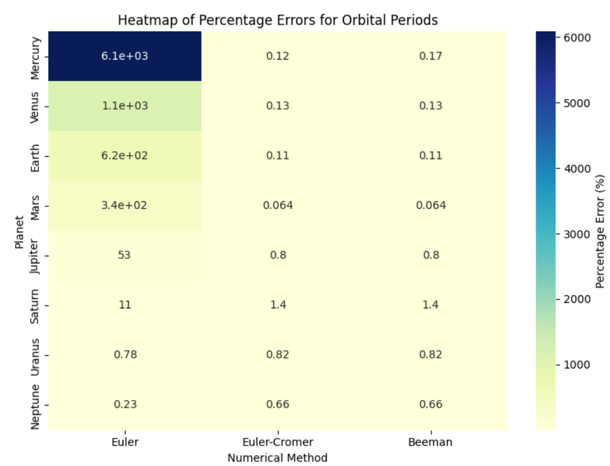

Figure 4: Heatmap of Percentage Errors for Orbital Periods. Darker shades correspond to higher deviations from the accepted orbital periods, indicating less accurate methods.

From these visualizations, we see that **Beeman** and **Euler–Cromer** remain accurate to within a few percent for nearly all planets, whereas the simpler **Euler** method can deviate significantly, especially for the fast orbiting inner planets like Mercury. These results reinforce the well-known advantage of higher-order integrators for orbital simulations.

3.4 Planetary Transitions or Alignments

An additional experiment involved detecting *planetary alignments*, defined when multiple planets share nearly the same polar angle (e.g., within $\pm 5°$). The simulation logs each time the inner planets fall within this threshold.

Table 3: Alignment events for a strict $\pm 5^\circ$ threshold. This simulation ran for 1000 years with $\Delta t = 0.001$ years, starting all inner planets on the $+x$ axis ($y = 0$). Columns show the event index (#), the alignment time (yr), and the time Δt since the previous alignment.

#	Alignment Time (yr)	Δt (yr)
1	0.000	–
2	512.153	512.153
3	559.098	46.945
4	606.128	47.030
5	771.511	165.383
6	818.517	47.006
7	843.022	24.505
8	924.904	81.882
9	960.571	35.667
10	983.882	23.311
11	984.969	1.087

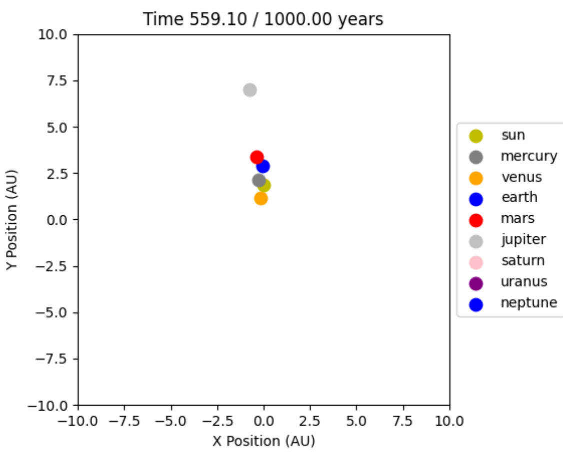

Figure 5: A sample alignment detection event ($t = 559.10$ years).

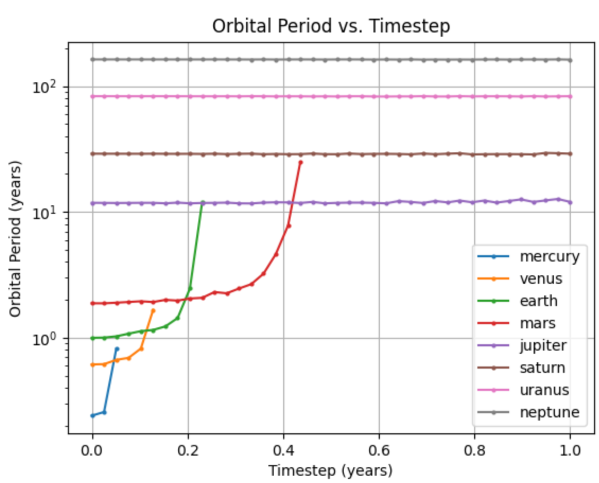

Figure 6: Orbital periods for planets as a function of the integration timestep. The vertical axis (log scale) displays the first detected orbital period (in years) for each planet. Inner planets exhibit a marked increase in deviation once Δt surpasses a fraction of their orbital period.

3.5 Impact of Timestep on Orbital Periods

As shown in Figure 6, the *first detected orbital period* of each planet is highly sensitive to the chosen timestep, particularly for the inner planets with tighter orbits. When Δt becomes large relative to an inner planet's orbital timescale, the simulation accumulates significant errors, causing the reported period to diverge from the expected physical value. In contrast, outer planets (which have much longer orbital periods and experience weaker accelerations) exhibit more stable orbital period measurements over a broader range of timesteps. This highlights the trade-off between computational efficiency (larger Δt) and simulation accuracy, especially for planets with short periods.

4 Discussion

Beeman's method consistently outperformed the other two in nearly every metric. Its second-order accuracy led to orbital periods that closely matched accepted reference values, with errors remaining below 1% for most planets. Moreover, standard deviations of these periods were minimal, typically under 0.01 years, indicating that the orbits remained stable over a 2000-year simulation span.

In contrast, the Euler method introduced significant deviations in orbital behavior, especially for inner planets like Mercury and Venus. The errors compounded over time, resulting in high variance and artificial alignment events that do not reflect physical reality. Euler-Cromer offered a significant improvement over Euler, demonstrating much better orbital consistency and energy conservation, although still slightly inferior to Beeman in precision.

Energy drift and oscillation metrics further reinforced these findings. Beeman minimized both long-term drift and short-term fluctuations in total energy, while Euler showed substantial degradation. The heatmaps and time-series energy plots made these differences immediately apparent and served as visual evidence for method comparison.

5 Conclusions

This project evaluated the effectiveness of three integration schemes, Euler, Euler-Cromer, and Beeman in simulating many-body orbital dynamics over a 2000-year period. Beeman's method consistently delivered the most accurate and stable results, closely replicating reference orbital periods, conserving total energy, and maintaining low variance across successive orbits. Euler-Cromer followed closely, offering a simpler implementation while still achieving reliable accuracy.

By contrast, the Euler method suffered from significant numerical instability, leading to large energy drifts, inconsistent orbital periods. These results were especially pronounced for fast-orbiting inner planets, where precise timestep integration is critical.

The simulation results clearly demonstrate that higher-order integrators such as Beeman are essential for achieving physically meaningful outcomes in long-term celestial mechanics modeling. They preserve both the qualitative behavior and quantitative metrics of the system over extended periods.

Future extensions of this work may include additional bodies or moons, or applications to dynamically active exoplanetary systems. Such improvements would allow further validation of integrators under even more complex gravitational interactions.